A store-operated nonselective cation channel in lymphocytes is activated directly by Ca2+ influx factor and diacylglycerol

Zhengchang Su, Peter Csutora, Dacia Hunton, Richard L. Shoemaker, Richard B. Marchase and J. Edwin Blalock

Am J Physiol Cell Physiol 280:1284-1292, 2001.

Am J Physiol Cell Physiol
280: C1284–C1292, 2001.

A store-operated nonselective cation channel in lymphocytes is activated directly by Ca^{2+} influx factor and diacylglycerol

ZHENGCHANG SU,[1] PETER CSUTORA,[2] DACIA HUNTON,[2] RICHARD L. SHOEMAKER,[1] RICHARD B. MARCHASE,[2] AND J. EDWIN BLALOCK[1]
[1]*Departments of Physiology and Biophysics and* [2]*Department of Cell Biology, Schools of Medicine and Dentistry, University of Alabama at Birmingham, Birmingham, Alabama 35294*

Received 1 August 2000; accepted in final form 11 December 2000

Su, Zhengchang, Peter Csutora, Dacia Hunton, Richard L. Shoemaker, Richard B. Marchase, and J. Edwin Blalock. A store-operated nonselective cation channel in lymphocytes is activated directly by Ca^{2+} influx factor and diacylglycerol. *Am J Physiol Cell Physiol* 280: C1284–C1292, 2001.—Agonist-receptor interactions at the plasma membrane often lead to activation of store-operated channels (SOCs) in the plasma membrane, allowing for sustained Ca^{2+} influx. While Ca^{2+} influx is important for many biological processes, little is known about the types of SOCs, the nature of the depletion signal, or how the SOCs are activated. We recently showed that in addition to the Ca^{2+} release-activated Ca^{2+} (CRAC) channel, both Jurkat T cells and human peripheral blood mononuclear cells express novel store-operated nonselective cation channels that we termed Ca^{2+} release-activated nonselective cation (CRANC) channels. Here we demonstrate that activation of both CRAC and CRANC channels is accelerated by a soluble Ca^{2+} influx factor (CIF). In addition, CRANC channels in inside-out plasma membrane patches are directly activated upon exposure of their cytoplasmic side to highly purified CIF preparations. Furthermore, CRANC channels are also directly activated by diacylglycerol. These results strongly suggest that the Ca^{2+} store-depletion signal is a diffusible molecule and that at least some SOCs may have dual activation mechanisms.

capacitive calcium entry; second messenger; ion channel

UPON AGONIST BINDING, numerous receptors in the plasma membrane activate phospholipase C (PLC) (1, 5), which cleaves phosphatidylinositol 4,5-bisphosphate into 1,2-diacylglycerol (DAG) and inositol 1,4,5-trisphosphate (IP_3). Binding of IP_3 to its receptors on internal Ca^{2+} stores such as the endoplasmic reticulum (ER) releases sequestered Ca^{2+} into the cytosol. Such depletion of Ca^{2+} stores gives rise to a signal that activates Ca^{2+}-permeable channels in the plasma membrane, allowing sustained Ca^{2+} (24), and in some cases Na^+ (10, 18, 29), influx into the cytosol from the extracellular space. This Ca^{2+} entry has been termed capacitative Ca^{2+} entry (CCE), with the responsible plasma membrane channels being referred to as store-operated channels (SOCs) (5, 24). While Ca^{2+} and Na^+ influxes are important for many biological processes, little is known about the nature of the depletion signal or the mechanism of activation of SOCs.

Establishing whether a diffusible depletion signal is responsible for CCE has been slowed by the lack of both a rich source of the material and a well-characterized SOC with measurable unitary conductance that is not spontaneously activated during whole cell and excised patch recordings. We previously demonstrated that extracts of *pmr1*, a yeast mutant with a genetically disrupted ER Ca^{2+}-ATPase (27), contains a diffusible Ca^{2+} influx factor (CIF) that accelerates the spontaneous activation of Ca^{2+} release-activated Ca^{2+} (CRAC) channels in Jurkat T cells during whole cell recordings (6). It was recently found (Su Z, Guo X, Shoemaker RL, Marchase RB, and Blalock JE, unpublished observations) that Jurkat T cells as well as human peripheral blood mononuclear cells (PBMCs), in addition to CRAC channels, express novel Ca^{2+}-conducting SOCs termed Ca^{2+} release-activated nonselective cation (CRANC) channels (15). The CRANC channel in Jurkat T cells and PBMCs has a relatively large single-channel conductance of 18–27 pS (average 23.1 pS) and is not activated by dialysis of the cytosol during whole cell recordings. These properties make the CRANC channel a good candidate for the characterization of CIF as well as for the study of the activation mechanism for SOCs.

In the present study we have further purified CIF from the *pmr1* yeast mutant by high-performance liquid chromatography (HPLC) and have shown that a single fraction accelerates the onset of current conducted by CRAC channels (I_{CRAC}) in the whole cell configuration and directly activates isolated CRANC channels in inside-out plasma membrane patches. We also have found that CRANC channels can be activated in a membrane-delimited manner by a DAG analog. This finding suggests that certain Ca^{2+}-permeable channels may be dually regulated by both second messengers and store depletion. In addition, the finding of a channel that is activated in a membrane-delimited way by a CIF further strengthens the notion that the Ca^{2+} store-depletion signal is a diffusible molecule.

Address for reprint requests and other correspondence: J. E. Blalock, Dept. of Physiology and Biophysics, Univ. of Alabama at Birmingham, 1918 Univ. Blvd. MCLM 898, Birmingham, AL 35294-0005 (E-mail: blalock@uab.edu).

The costs of publication of this article were defrayed in part by the payment of page charges. The article must therefore be hereby marked "*advertisement*" in accordance with 18 U.S.C. Section 1734 solely to indicate this fact.

MATERIALS AND METHODS

Cell culture. Jurkat T and rat basophilic leukemia (RBL-2H3) cells were from American Type Culture Collection (Rockville, MD). Jurkat T cells were maintained at 37°C in 5% CO_2 in RPMI 1640 media (Sigma, St. Louis, MO) with the following substitutions (Mediatech, Herndon, VA): 10% heat-inactivated fetal calf serum, 10,000 IU/ml penicillin, 10,000 μg/ml streptomycin, 2 mM glutamine, 10 mM sodium pyruvate, 10 mM nonessential amino acid, and 25 mM HEPES. RBL-2H3 cells were maintained in MEM (Sigma)-based media, as previously described (19).

CIF preparation and HPLC fractionation. Acid extracts from wild-type and *pmr1* yeast cells were prepared as described previously (6). After centrifugal ultrafiltration through Biomax-30 Ultrafree-MC filters (Millipore, Bedford, MA), the crude extracts were loaded onto a Partisil 10 strong anion exchange HPLC column (Keystone Scientific, Bellefonte, PA). After a 10-min isochratic lag at a flow rate of 2 ml/min, a 40-min linear salt and pH gradient was applied from 5 to 750 mM $(NH_4)H_2PO_4$ and from pH 2.8 to 3.7, respectively. The activity was reconstituted from fractions with retention times of 22.5–24 min. Before electrophysiological recordings were performed, the activity of the fractions was screened by microinjection into fura 2-loaded albino *Xenopus laevis* oocytes as described previously (6). Changes in intracellular Ca^{2+} concentration ($[Ca^{2+}]_i$) were measured on an Olympus IX70 inverted microscope (Lake Success, NY) through a ×10 UplanAPO objective, NA 0.17, equipped with a rapid excitation filter changer alternating between 340 and 380 nm (Ludl Electronics, Hawthorne, NY) and a charge-coupled device camera (Sensys, Photometrics, Tucson, AZ). Fluorescence increases were analyzed using the ratio extension of the IP-Lab Spectrum imaging software (Signal Analytics, Vienna, VA). Data are expressed relative to the 340/380 ratio at *time 0*.

Electrophysiological recordings. Conventional whole cell recordings were performed as described previously (6). Briefly, the standard pipette solution contained (in mM) 110 Cs-glutamate, 10 CsCl, 2.9 $MgCl_2$, 0.6 $CaCl_2$, 10 EGTA-Cs, and 30 HEPES, with pH 7.2 adjusted with CsOH and a calculated free $[Ca^{2+}]$ of 10 nM. The standard external solution consisted of (in mM) 143 NaCl, 10 $CaCl_2$, 1 $MgCl_2$, 4.5 KCl, 5 D-glucose, and 10 HEPES, with pH 7.3 adjusted with NaOH. The fast and slow capacitative transients were canceled, and a tip junction potential of +10 mV was not corrected. Series resistances (5–20 mΩ) were not compensated. After the whole cell configuration was achieved, the cells were held at −40 mV, and the signal was sampled at 5 kHz by applying a 320-ms voltage ramp from −100 to +100 mV at a frequency of 0.2 or 1 Hz. In some experiments the signal was digitized at 100 kHz and recorded on a magnetic tape. The signal was filtered at 1 kHz with an eight-pole low-pass Bessel filter (model 900; Frequency Devices, Haverhill, MT). The currents measured at −40 or −80 mV are displayed as indicated in the figure legends.

For inside-out patch recordings, the pipettes were filled with an external solution in which 10 mM $CaCl_2$ in the standard external solution was replaced by equimolar $MgCl_2$. Before the switch from the cell-attached to the inside-out configuration, the bath solution was changed to the standard internal solution. The signal was digitized at 100 kHz, recorded on a magnetic video tape, and analyzed off-line. For analysis, the signal was resampled at 5 or 10 kHz and filtered at 300 Hz by the eight-pole low-pass Bessel filter. Voltage ramps from −100 to +100 mV in 320 ms were applied to the inside-out patches to obtain the single-channel current-voltage (*I-V*) relationship. In some experiments the single-channel *I-V* relationship was obtained by holding the cell at various voltages. Unitary current was determined by amplitude histogram analysis using pCLAMP 6 (Axon Instruments, Foster City, CA).

Materials. Thapsigargin (TG) and ionomycin were purchased from Calbiochem (La Jolla, CA). DAG analog 1-oleoyl-2-acetyl-*sn*-glycerol (OAG) and the salts were from Sigma.

Data analysis. The activation time course of CRAC channels was fitted to the equations $I = I_0 + I_1 \cdot \exp[-(t - t_{delay})/\tau]$ or $I = I_0 + I_1 \cdot \exp[-(t - t_{delay})/\tau_1] + I_2 \cdot \exp[-(t - t_{delay})/\tau_2]$, where I is the current, t is time, I_0, I_1, and I_2 are constants, τ, τ_1, and τ_2 are activation time constants, and t_{delay} is the time when the current develops to 10% of the maximum level after whole cell break-in. Data are shown as means ± SE, and the *t*-test was used for statistical analysis.

RESULTS

CIF-containing extracts from pmr1 yeast accelerate the spontaneous activation of the CRAC channel in RBL-2H3 cells. We have previously shown that CIF preparations from the *pmr1* yeast mutant can activate Ca^{2+} entry in *Xenopus* oocytes and accelerate activation of CRAC channels when included in the pipette solution during whole cell dialysis of Jurkat T cells (6). The latter finding was confirmed in RBL-3H3 cells (Fig. 1, *A* and *B*), because inclusion of a crude extract of *pmr1* CIF in the whole cell pipette solution (1:100 dilution) significantly ($P < 0.001$) accelerated the spontaneous activation of CRAC channels (t_{delay} = 8.9 ± 2.3 s, n = 5) compared with that seen when the pipette solution contained extract from wild-type yeast at the same dilution (t_{delay} = 47.5 ± 15.6 s, n = 5). In addition, when CIF was not present in the pipette solution, the time course of the I_{CRAC} activation was biphasic and could be fitted by a two-component exponential equation with time constants τ_1 = 148.1 ± 23.4 s (n = 5) and τ_2 = 112.5 ± 17.8 s (n = 5), respectively. The biphasic activation course of CRAC channel by whole cell passive dialysis was also recently reported by Fierro and Parekh (7). In contrast, when CIF was included in the pipette solution, the time course of the I_{CRAC} activation was characterized by only a fast phase with a time constant of 16.1 ± 5.2 s (n = 8). This result strongly suggests that CIF accelerates the spontaneous activation of the CRAC channel in RBL-2H3 cells as in the case of Jurkat T cells. Interestingly, CRANC channels were not seen in RBL-2H3 cells (n = 10) no matter how concentrated CIF was in the pipette.

To further enrich for the active component of the crude CIF-containing extract from the *pmr1* mutant, we used HPLC to fractionate the extracts (Fig. 1*C*). The CIF activity of each fraction was first tested in X*enopus* oocytes. *Fractions 23* and *24*, when injected into X*enopus* oocytes, elicited robust Ca^{2+} influx, while the flanking *fractions 22, 25,* and *26* had no effect (Fig. 1*D*). In the absence of extracellular Ca^{2+}, injection of *fraction 24* into X*enopus* oocytes failed to induce $[Ca^{2+}]_i$ elevation, suggesting that CIF-induced $[Ca^{2+}]_i$ elevation is due to Ca^{2+} influx (Fig. 1*D*).

Consistent with the supposition of a single active species, *fractions 23* and *24*, when included in the

whole cell pipette solution in RBL-2H3 cells, accelerated the activation of I_{CRAC} [t_{delay} = 5.2 ± 2.4 s (n = 6) and 5.1 ± 3.6 s (n = 6) for *fractions 23* and *24*, respectively] and changed the activation time course of the CRAC channel from biphasic to monophasic [τ = 31.3 ± 7.2 s (n = 6) and 21.8 ± 6.8 s (n = 6) for *fractions 23* and *24*, respectively] (Fig. 1*E*). In contrast, the subsequent *fractions 25* and *26* did not have this capability. As shown in Fig. 1*E*, when *fractions 25* or *26* were included in the whole cell pipette solution, the activation time course of I_{CRAC} was biphasic with τ_1 = 80.1 ± 13.8 and 76.3 ± 11. 3 s, τ_2 = 68.4 ± 5.9 and 70.9 ± 8.5 s, and t_{delay} = 35.2 ± 5.2 and 35 ± 6.7 s, respectively (n = 6 for both *fractions 25* and *26*), which is not significantly different ($P > 0.1$) from that when the pipette solution contained wild-type yeast extracts [τ_1 = 87.7 ± 9.6 s, τ_2 = 76.3 ± 6.9 s, and t_{delay} = 31.5 ± 5.6 s (n = 14)].

CIF-containing extracts from pmr1 yeast activate CRANC channels. It was recently demonstrated (Su Z, Guo X, Shoemaker RL, Marchase RB, and Blalock JE, unpublished observations) that CRANC channels in Jurkat T cells are activated by depletion of internal Ca^{2+} stores. Therefore, we tested the effects of CIF preparations on CRANC channel activation. When lower doses (1:300–500) of crude CIF were included in the pipette solution, the current conducted by the CRANC channel (I_{CRANC}) was not activated (data not shown), although this dose was sufficient to accelerate the spontaneous activation of CRAC channels in these cells (6). However, when an intermediate dose of crude CIF extract (1:100) was included in the pipette, a small current with an inwardly rectifying *I-V* relationship and a positive reversal potential (*I-V* curve not shown), which are characteristics of the CRAC channel, was rapidly activated (Fig. 2A). Subsequently, a second, larger current became apparent. This current had properties consistent with it being carried by the recently described CRANC channel (Su Z, Guo X, Shoemaker RL, Marchase RB, and Blalock JE, unpublished observations), as indicated by a shift of the reversal potential toward −15–0 mV and an outwardly rectified *I-V* relationship (see below). The sequential activation of CRAC and then CRANC channels by the intermediate dose of CIF would appear to reflect their different sensitivities to CIF as its intracellular concentration increases.

When included in the pipette solution at a still higher dose (1:30 dilution), crude CIF extracts from the *pmr1* mutant rapidly activated an inward conductance

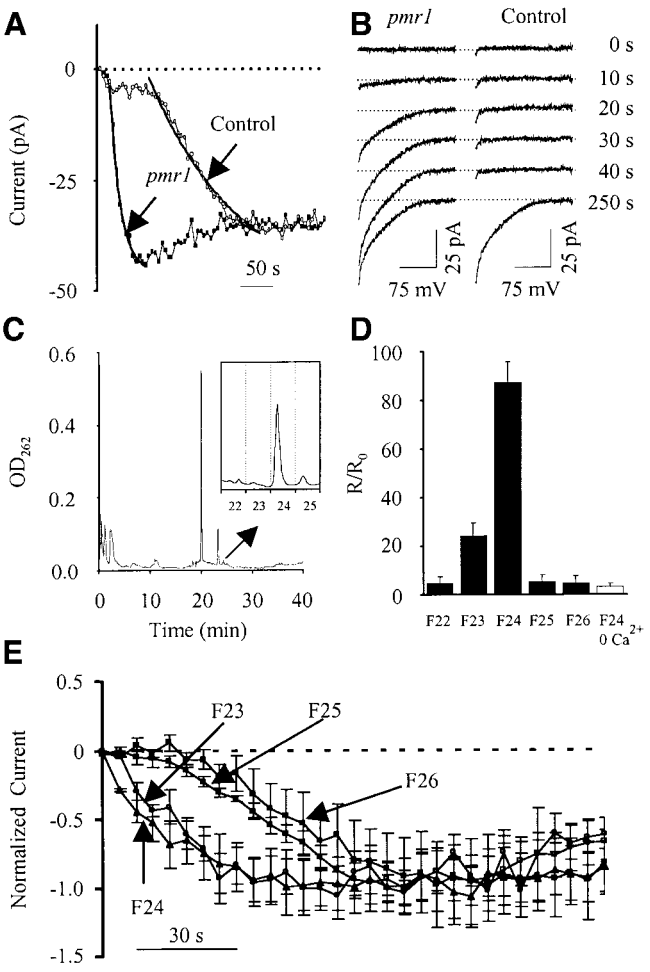

Fig. 1. Ca^{2+} influx factor (CIF)-containing *pmr1* extracts accelerate the activation of the Ca^{2+} release-activated Ca^{2+} (CRAC) channel in RBL-2H3 cells. *A*: whole cell current measured at −80 mV was plotted as a function of time after whole cell break-in. This is a representative experiment of 5 such paired replicates. In this experiment the 2 cells have the same size and same steady-state current. However, inclusion of CIF-containing *pmr1* extracts (1:100) in the pipette solution greatly accelerated the activation of CRAC current (I_{CRAC}; t_{delay} = 10 s) compared with the control cell, in which the pipette solution contained wild-type yeast extract at the same dilution (t_{delay} = 60 s). The activation time course of I_{CRAC} when the pipette solution contained *pmr1* extracts can be fitted to a 1-component exponential equation with τ = 16 s. In contrast, the activation time course of I_{CRAC} when the pipette solution contained wild-type yeast extracts can be fitted by a 2-component exponential equation with τ_1 = 140 s and τ_2 = 127 s. *B*: representative current-voltage (*I-V*) curves of the currents taken from the *pmr1* and wild-type yeast extract-treated cells from the experiment shown in *A* at the indicated times. The *I-V* curves were generated by applying voltage ramps from −100 to 100 mV in 320 ms. *C*: HPLC anion exchange chromatogram of an acid extract prepared from 100 OD_{600} units of *pmr1* yeast cells. *Inset*: expanded view of a portion of the chromatogram between 22 and 25 min of retention time. *D*: increases in fluorescence ratio after microinjection of HPLC *fractions 22–26* of *pmr1* yeast extract into fura 2-loaded *Xenopus* oocytes. The data refer to the maximal R/R_o averaged over a 500 × 700-μm area containing ~45% of the oocyte, including the injection site, 6 min after injection. External [Ca^{2+}] was 5 mM except for the experiment depicted by an open bar, in which the medium surrounding the oocyte was nominally Ca^{2+} free. Data are means ± SD from 3–8 replicates. *E*: whole cell current in RBL-2H3 cells measured at −80 mV and normalized to the maximum current of each cell. Each data point represents means ± SE pooled from 6 cells. When *fractions 23* and *24* were included in the whole cell pipette solution, the activation of CRAC channels in the RBL-2H3 cells was accelerated (t_{delay} = 5.2 ± 2.4 and 5.1 ± 3.6 s, respectively). The activation time course could be fitted to a 1-component exponential equation (τ = 31.3 ± 7.2 and 21.8 ± 6.8 s for *fractions 23* and *24*, respectively). In contrast, when *fractions 25* and *26* were included in the pipette solution, the activation course of the CRAC channel could be fitted to a 2-component exponential equation that is not different from that when the pipette solution contained wild-type yeast extracts. The fitting and control data are not shown for clarity.

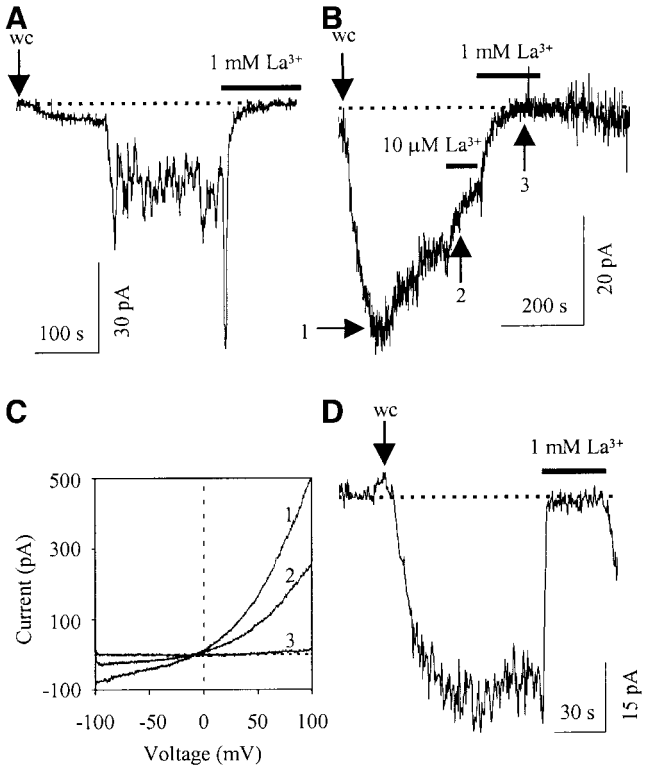

Fig. 2. CIF-containing *pmr1* extracts activate the Ca^{2+} release-activated nonselective cation (CRANC) channel in Jurkat T cells. Whole cell break-in is indicated by arrows labeled wc, and the current displayed was measured at −40 mV. *A*: inclusion of an intermediate dose (1:100) of CIF-containing *pmr1* extract in the whole cell pipette solution first activated CRAC and then CRANC channels as indicated by their current size and *I-V* curves (not shown). *B*: inclusion of a high dose of CIF-containing *pmr1* extracts (1:30) in the whole cell pipette solution activated the CRANC channel after whole cell break-in. The current was partially sensitive to 10 μM La^{3+} but was completely blocked by 1 mM La^{3+}. Numbered arrows indicate the time points at which *I-V* curves were taken and are plotted in *C*. *D*: inclusion of *fraction 24* (1:100 dilution) in the whole cell pipette solution activated CRANC channels in a Jurkat T cell as indicated by *I-V* curves (not shown) and the sensitivity of the current to 1 mM La^{3+}.

following whole cell break-in (Fig. 2*B*). The *I-V* relationship (Fig. 2*C*) again suggests that the current was conducted by a nonselective cation channel and was observed in 56% (28/50) of Jurkat T cells tested at high CIF doses (1:30–50 dilution). The nonselective conductance activated by the crude CIF extracts was only partially sensitive to 10 μM La^{3+} and fully sensitive to 1 mM La^{3+} (Fig. 2*B*). The conductance showed an outwardly rectifying *I-V* curve with a reversal potential of −15–0 mV (Fig. 2*C*), all characteristics resembling those of the I_{CRANC} activated by TG, IP_3, or ionomycin (Su Z, Guo X, Shoemaker RL, Marchase RB, and Blalock JE, unpublished observations).

The HPLC fractions assessed in RBL-2H3 cells were also tested in Jurkat cells. *Fraction 24*, when included in the whole cell pipette solution, also activated I_{CRANC} in 53% (13/25) of the Jurkat T cells tested (Fig. 2*D*). Similar potency was observed for *fraction 23* but not for *fractions 25* and *26* (data not shown). Together, these results strongly suggest that CIF can serve as a universal depletion signal to activate different types of SOCs.

CRANC channels are activated by CIF in a membrane delimited fashion. As was described recently (Su Z, Guo X, Shoemaker RL, Marchase RB, and Blalock JE, unpublished observations), CRANC channels in isolated patches do not remain active upon patch excision. We therefore were able to test the direct effect of CIF from *pmr1* mutant yeast on CRANC channels in Jurkat T cells in the inside-out configuration. As shown in Fig. 3, when 10 mM Mg^{2+} was included in the pipette solution to block CRAC channels, the switch from the cell-attached to the inside-out configuration did not activate any channel activity (Fig. 3*A*). However, application of a *pmr1* mutant extract (1:30 dilution) to the cytoplasmic side of the inside-out patch activated an inward conductance (Fig. 3*B*) with a unitary current of 1.5 ± 0.3 pA (n = 5) at a holding potential of −65 mV as determined by amplitude histogram analysis (Fig. 3*H*). Perfusion of the cytoplasmic side of the patch for ~3 min in the absence of CIF abolished the channel activity (Fig. 3*C*), but reapplication of the CIF-containing preparation to the cytoplasmic side of the patch reactivated the channel (Fig. 3*D*). These results show that the conductance is activated in a membrane-delimited manner by CIF, possibly by binding to the cytoplasmic side of the channel. HPLC *fractions 23* and *24* had the same effects, but *fractions 25* and *26* did not (data not shown). The *I-V* curve of a single channel activated by CIF is outwardly rectified with a reversal potential of around −15–0 mV (Fig. 3, *E* and *F*). Linear fitting of the single channel *I-V* curves in the negative holding potential region yields a unitary chord conductance of 23.4 ± 0.4 pS (n = 4) (Fig. 3*G*), which is similar to that of CRANC channel activated by depletion of Ca^{2+} stores. Even though this patch contained only one channel, as in the case of TG or ionomycin (Su Z, Guo X, Shoemaker RL, Marchase RB, and Blalock JE, unpublished observations), CIF more often activated multiple channels in the patches (16/20; data not shown).

CRANC channels are activated directly by DAG, and TRP3 and/or TRP6 are likely components of the CRANC channels. It has been shown that Jurkat T cells express high levels of mRNAs for TRP3 and TRP6 transient receptor potential proteins, whereas RBL cells express no mRNAs for TRP3 and a low level of mRNAs for TRP6 (8). Both TRP3 and TRP6, when expressed heterologously, form a nonselective cation channel with biophysical properties similar to those of the CRANC channel that have been described (Su Z, Guo X, Shoemaker RL, Marchase RB, and Blalock JE, unpublished observations). Interestingly, Hofmann and coworkers (11) recently showed that either TRP3 or TRP6 channels can be directly activated by DAG. When Jurkat T cells were tested in whole cell recordings, membrane-permeable DAG analog OAG activated an inward current (Fig. 4*A*) that had a slightly outwardly rectifying *I-V* curve (Fig. 4*B*), with a rever-

sal potential of −15–0 mV, that was partially sensitive to 10–20 μM La^{3+} (data not shown) and that could be completely blocked by 1–2 mM La^{3+}. Furthermore, after CRANC channels were fully activated by inclusion of CIF in the whole cell pipettes, application of OAG to the cells could not activate any additional current (n = 8) (Fig. 4*C*). All these properties suggest that the current activated by OAG is carried by CRANC channels. We next asked whether OAG could activate the CRANC channel in a membrane-delimited manner in inside-out patches. As shown in Fig. 5*A*, application of 100 μM OAG to the cytoplasmic side of an inside-out patch from a Jurkat T cell immediately activated an inward current. Amplitude histogram analysis (Fig. 5*B*) revealed that the current was conducted by multiple channels with the same unitary current of 1.5 ± 0.3 pA (n = 3) at a holding potential of −65 mV (Fig. 5*C*), suggesting that these channels were the same type. The channel activity could not be completely abolished by extensive washing of the cytoplasmic side of the patch. The single-channel *I-V* curve of this channel was also slightly outwardly rectifying with a reversal potential near 0 mV (Fig. 5, *D* and *E*).

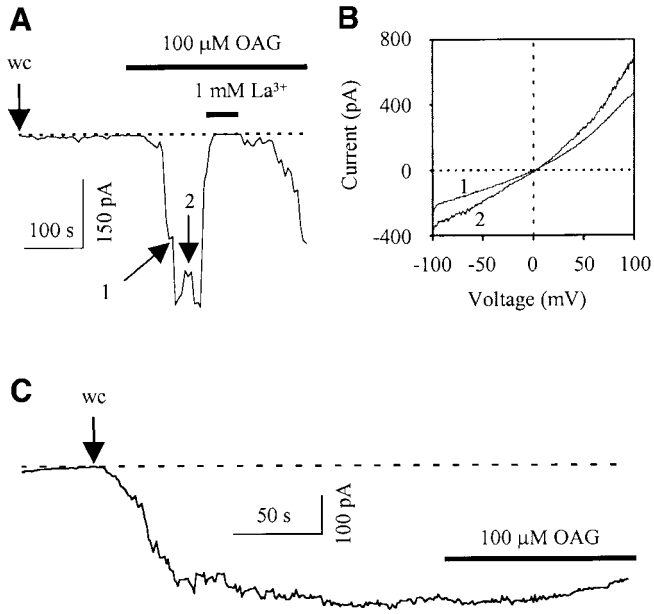

Fig. 4. Diacylglycerol (DAG) activates the CRANC channel. *A*: application of the DAG analog 1-oleoyl-2-acetyl-*sn*-glycerol (OAG; 100 μM) to a Jurkat T cell activated CRANC channels in the whole cell configuration, as suggested by the *I-V* curves of the current taken at the time points indicated by the numbered arrows and shown in *B*. The current was measured at −80 mV. *C*: the whole cell pipette contained partially purified CIF (1:30). After I_{CRANC} was fully activated, application of 100 μM OAG failed to activate any additional current (n = 8).

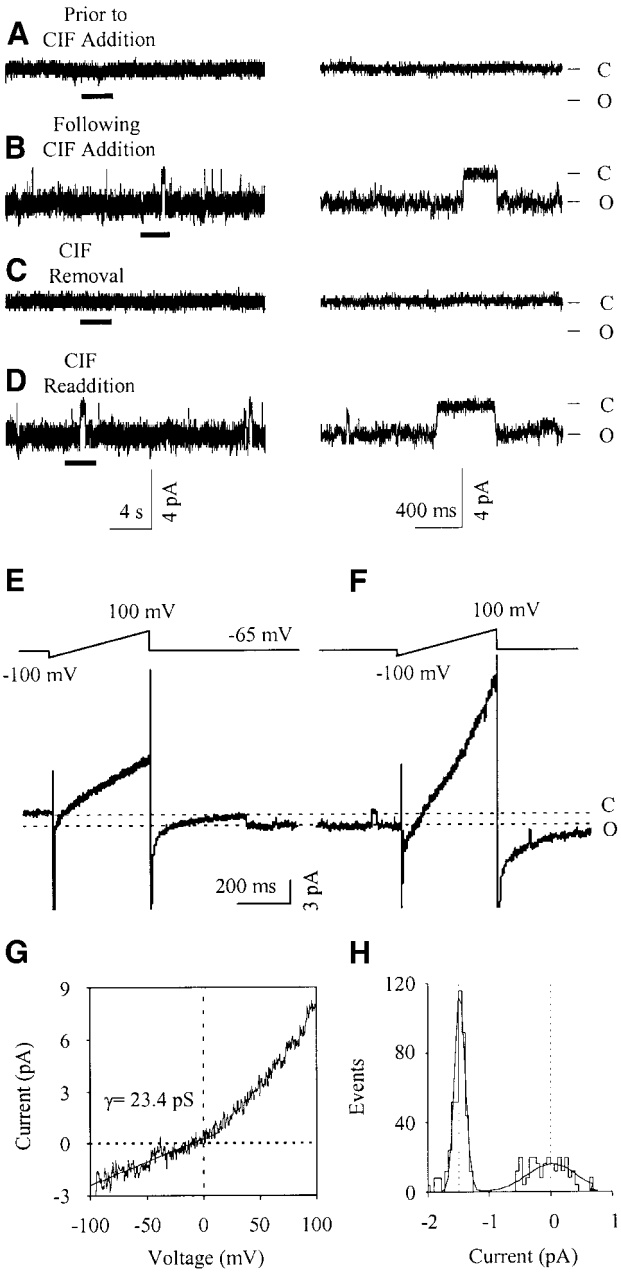

Fig. 3. CIF directly activates CRANC channels in inside-out patches from Jurkat T cells. Inside-out patches were held at −65 mV. The solutions used in this experiment are described in MATERIALS AND METHODS. *A–D*: *right traces* are expanded displays of the segment indicated by a horizontal bar in *left traces*. C and O indicate closed and open states of the channel, respectively. All data were collected from the same cell. *A*: after switching from the cell-attached to an inside-out patch configuration and before CIF addition, no channel activity was seen. *B*: addition of CIF-containing *pmr1* extracts (1:30 dilution) into the recording chamber activated an inward conductance. *C*: extensive washing of the cytoplasmic side of the patch abolished the channel activities. *D*: readdition of CIF-containing *pmr1* extracts reactivated the channel. *E*: after the channel was activated by applying CIF to the cytoplasmic side of the patch, a 320-ms voltage ramp from −100 to +100 mV was applied from a holding potential of −65 mV to obtain the single-channel *I-V* curve. Representative trace of recordings shows where the channel remained in the closed state when the voltage ramp was applied. *F*: representative trace of recordings shows where the channel remained in the open state while the voltage ramp was applied. *G*: the unitary *I-V* curve of the channel was obtained by subtracting the leak current invoked by the voltage ramp in *E* from the current invoked by the voltage ramp in *F*. The unitary conductance is 23.4 pS in the negative voltage region. *H*: current amplitude histogram analysis shows that the patch contains a single channel. The smooth line is Gaussian fitting of the data, which yields a unitary current of 1.5 pA ± 0.3 (n = 5).

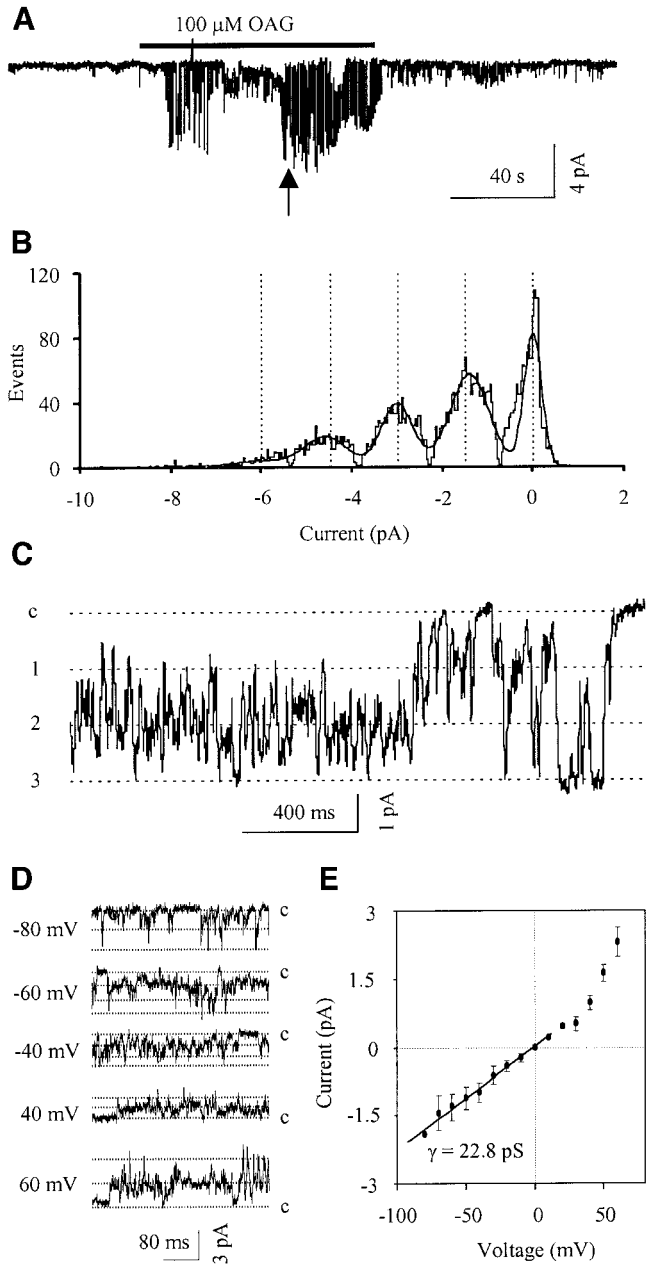

Fig. 5. CRANC channels were activated by OAG in a membrane-delimited manner. *A*: after switching to the inside-out patch configuration, the patch was held at −65 mV. Application of OAG (100 μM) to the cytoplasmic side of the patch activated an inward current. Washing out the OAG in the chamber could not completely abolish the channel activities. *B*: current amplitude histogram analysis of the current in *A*. The smooth line is Gaussian fitting of the data, which yield a unitary current of 1.5 ± 0.3 pA (n = 3). *C*: expanded display of the recording point indicated by the arrow in *A*, showing the channel activities in the presence of OAG. Three levels of channel opening with a unitary current of 1.5 pA can be seen at this point. *D*: representative traces of OAG-activated currents recorded at various holding potentials in an inside-out patch taken from another cell. *E*: the *I-V* relationship of OAG-activated channel. Linear fitting of the *I-V* curve at the negative voltage region yields a chord unitary conductance of 22.8 ± 1.0 pS (n = 3).

Linear fitting of this *I-V* curve in the negative holding potential region yields a unitary chord conductance of 22.8 ± 1.0 pS (Fig. 5*E*, n = 3), which is similar to that of the CRANC channel activated by TG (Su Z, Guo X, Shoemaker RL, Marchase RB, and Blalock JE, unpublished observations) and CIF, suggesting again that OAG can directly activate the CRANC channel. Although CIF and OAG likely activate the same CRANC channel, on the basis of the single-channel conductance and slightly outwardly rectified *I-V* relationship the mechanism of activation is clearly different. This is easily observed on the basis of the difference in open time and the apparent lack of reversibility of OAG activation (Fig. 5).

To investigate the relationship between the CRANC channel and TRP3 and/or TRP6, we tested the effects of OAG on the RBL cells in whole cell recordings. As shown in Fig. 6, *A* and *B*, after I_{CRAC} had been fully activated by dialysis of the cytosol, application of 100 μM OAG to the cells failed to activate any additional current; instead, it inhibited I_{CRAC} ~10.3 ± 1.4% (n = 8) by an unknown mechanism. This result, together with the above finding that even high doses of CIF fail to activate any nonselective cation current in RBL cells, suggests that these cells do not express CRANC channels. This is consistent with the previous report that RBL cells express no mRNAs for TRP3 or a very low level of mRNAs for TRP6 proteins (8). Together, the results shown here suggest that the CRANC channel in Jurkat T cells and human PBMCs may be at least partially assembled from TRP3 and/or TRP6 proteins.

DISCUSSION

The mechanism by which ER Ca^{2+} store depletion leads to an influx of extracellular Ca^{2+} remains clouded on at least two fronts. First, the nature of the signal transduction pathway by which store depletion is linked to the opening of plasma membrane Ca^{2+} channels remains controversial. Second, while it is clear that in different types of cells several types of ion channels are utilized for the depletion-mediated influx of Ca^{2+}, it has not been definitely shown that an

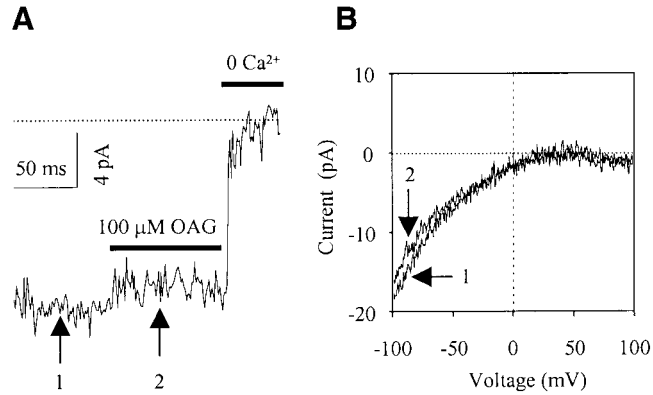

Fig. 6. OAG fails to activate a nonselective conductance in RBL cells. *A*: after I_{CRAC} was fully activated in whole cell configuration, application of 100 μM OAG to the cell could not activate any additional current; instead, it inhibited I_{CRAC} ~10.3% (n = 8). I_{CRAC} was completely blocked when extracellular Ca^{2+} was replaced with equimolar Mg^{2+} as indicated by the horizontal bar (0 Ca^{2+}). *B*: *I-V* curves of the current taken at the time points in *A* indicated by corresponding numbered arrows.

identified channel or subunit is responsible for a given native Ca^{2+} current.

With respect to the signal for Ca^{2+} store depletion, three not necessarily distinct models have been proposed. In one model, a static physical link between proteins at the surface of the ER, perhaps the IP_3 receptor, and a complex that includes the responsible plasma membrane Ca^{2+} channel is proposed (14, 16, 23). Changes in the conformation of the IP_3 receptor or another ER membrane protein resulting from the depletion of intracellular Ca^{2+} stores could activate the plasma membrane channel. In the second model, a role for interactions between secretory-like transport vesicles and the plasma membrane is proposed (20, 32). The vesicle could be important as a source for the insertion of channels previously not present in the plasma membrane or, via a mechanism in which vesicle fusion is not required but, rather, in which a transient physical interaction of vesicles with the plasma membrane surface activates resident plasma membrane channels, a so-called "kiss and run" mechanism. In the third model, it was postulated that a soluble second messenger-like molecule that is freely diffusible is formed by the ER upon Ca^{2+} store depletion. This molecule, termed Ca^{2+} influx factor (CIF) by Randriamampita and Tsien (25, 26), is predicted to activate channels either directly or through interaction with a closely associated regulatory protein.

In a previous study (6) we presented evidence that CIF, prepared from either TG-treated Jurkat cells or *pmr1* mutant yeast in which the organellar Ca^{2+} stores are disrupted by genetic manipulation (27), is able to activate Ca^{2+} influx in *Xenopus* oocytes. In addition, when the putative CIF was included in a patch pipette, the activation of I_{CRAC} in Jurkat cells was much more rapid than that achieved by passive dialysis or the inclusion of IP_3 in the pipette during whole cell recordings. These data suggest that a CIF exists and can activate the channel responsible for I_{CRAC}. Here, we have confirmed in whole cell patch-clamp experiments in RBL-2H3 cells that I_{CRAC} is activated in a rapid fashion by crude as well as more highly purified yeast CIF. In addition, we have shown that, in Jurkat T cells, the presence of a higher dose of CIF in the pipette leads to activation of another store-operated cation channel with a unitary conductance of 18–27 pS, which was termed CRANC channel (Su Z, Guo X, Shoemaker RL, Marchase RB, and Blalock JE, unpublished observations) in keeping with an earlier description of a similar channel found in mouse pancreatic acinar cells (15).

Perhaps the most rigorous test for the ability of the putative CIF to activate a channel comes from experiments with inside-out patches. Our attempts to examine the channels responsible for I_{CRAC} utilizing this technique have been thwarted by the finding that, once activated, the CRAC channel stays open in isolated patches (Su Z, Guo X, Shoemaker RL, Marchase RB, and Blalock JE, unpublished observations). The same phenomenon was observed for a SOC in *Xenopus* oocytes by Yao and coworkers (32). Moreover, the act of isolating the patch itself leads rapidly to an activation of I_{CRAC} (unpublished observations; also see Ref. 3). We interpret these data as suggesting that in the absence of the cytoplasmic environment, an inhibitory mechanism is lost from the CRAC channel and that the continuous presence of an activating agent such as CIF, after the irreversible loss of the inhibitory moiety, is no longer required. The finding that the CRANC channel in Jurkat T cells can only be activated by active depletion of internal Ca^{2+} stores and that its activation depends on the cellular environment of a depleted cell (Su Z, Guo X, Shoemaker RL, Marchase RB, and Blalock JE, unpublished observations) allows us to directly test the effect of the putative CIF on patches containing this channel. As shown in Fig. 3, this channel, when exposed on the cytoplasmic surface to partially purified CIF preparations, is activated with a conductance typical of the CRANC channel activated by ionomycin or TG in the cell-attached configuration (Su Z, Guo X, Shoemaker RL, Marchase RB, and Blalock JE, unpublished observations). This activation is reversible such that when the putative CIF was removed from the cytoplasmic surface of the patch, the current ceased.

These data suggest that two separate SOCs are activated by the presence of CIF and that the channels responsible for I_{CRAC} and those responsible for I_{CRANC} are regulated by two different mechanisms. CIF appears to activate the CRANC channel by binding to the cytoplasmic side of the channel or to a tightly associated regulatory molecule. In contrast, CIF may facilitate activation of CRAC channels by promoting the removal of an inhibitory mechanism that otherwise keeps the channel closed. Consistent with the results presented in this paper, an independent study with a mammalian preparation of CIF on isolated patches from rat aortic smooth muscle cells resulted in activation of a nonselective cation channel with a unitary conductance of 3 pS (30). Thus at least three SOCs are activated by CIF, albeit by different mechanisms.

Both Yao et al. (32) and Patterson et al. (20) recently presented evidence that implicated vesicle interactions with the plasma membrane as being important to the activation of capacitative Ca^{2+} entry. It is not yet clear how the results reported in those studies might be related to the data presented here. It is possible that vesicles or the ER capable of synthesizing CIF must be in close apposition to the plasma membrane to prevent a premature destruction of the active compound in the cytoplasmic milieu. Alternatively, the creation of a ring of actin-containing filaments near the surface of cells, shown to be inhibitory by Patterson et al. (20), could concentrate potential competitive binding sites for CIF and thus prevent it from reaching the cell surface. Another explanation could be that the formation of the F-actin cortex underneath the plasma membrane may prevent the disassociation of an inhibitory molecule from the channel.

In terms of the molecular identity of native SOCs, recent studies have implicated the mammalian homologues of the *Drosophila* TRP proteins as possible molecular components of SOCs. Although certain TRP

proteins, e.g., TRPL (34, 36), TRP4 (21), and TRP5 (22), form Ca^{2+}-selective SOCs when heterologously expressed, none of them alone shows the precise biophysical properties of CRAC channels. It has been shown that four types of *Drosophila* TRP homologues, TRP1, TRP3, TRP5, and TRP6, are expressed in Jurkat T cells (8). The CRANC channel recorded in lymphocytes most closely resembles TRP3 or TRP6 channels in terms of single-channel conductance (18–27 pS) and a slightly outwardly rectifying *I-V* relationship (2, 12, 33, 35). Recently, Hofmann et al. (11) showed that TRP3 or TRP6 channels can be directly activated by DAG in a membrane-delimited manner. Our finding that OAG directly activates the CRANC channels suggests that TRP3 and/or TRP6 is likely a subunit of the CRANC channel in Jurkat T cells. This notion is further strengthened by the finding that RBL cells have been shown previously to express no detectable or very low levels of mRNAs for TRP3 and TRP6, respectively (8), and do not express CRANC channels. Nofer and coworkers (17) also recently reported that a membrane-permeable DAG analog activates a nonselective cation channel in human lymphocytes mediating both Ca^{2+} and Na^{+} influxes. In other work, they found that this channel is also activated by arachidonic acid (AA) (18). The cation influx pathway they described is most likely the CRANC channel.

The polarity of CIF as well as its reversible effect on the CRANC channel excludes the possibility that DAG or AA is the active component in the CIF we are studying. Instead, the finding that CRANC channels can be activated by DAG or AA and CIF suggests a dual-activation mechanism for some SOCs. This dual-regulation mechanism is not unique for the CRANC channel. Chyb et al. (4) recently showed that both *Drosophila* TRP and TRPL channels can also be activated by polyunsaturated fatty acids such as linolenic acid and AA, even though the TRP channel has also been shown to be store operated (9, 31). Kiselyov and Muallem (13) recently reported that linolenic acid, when applied to the cytoplasmic side of a patch, activates the TRP3 channel, probably through binding to the same site on the channel as DAG. Another AA derivative, 5,6-epoxyeicosatrienoic acid, also has been shown to activate capacitative Ca^{2+} entry in rat astrocytes (28). Because DAG and a depletion signal such as CIF are products of the activation of PLC-β or PLC-γ signaling pathway, a question is raised as to how these two signals coordinate with each other to regulate SOCs under physiological conditions. A detailed analysis of the relationship between CIF and DAG in the activation of CRANC channels may help to answer this question.

The data presented here thus show that a small molecular weight molecule, enrichable by chromatography and present in cells depleted of ER Ca^{2+} but not in control cells, is able to directly activate the CRANC channel in isolated patches taken from Jurkat T cells. This fraction is also capable of facilitating the activation of I_{CRAC} in whole cell patch experiments. It also activates Ca^{2+} entry in *Xenopus* oocytes. Perhaps most importantly, the results demonstrate that CIF can activate the CRANC channel in a membrane-delimited fashion in isolated patches. This would appear to be particularly strong evidence for the existence of CIF and should be a technological advance that facilitates the identification of this compound. While the physiological role that CIF plays in vivo in Ca^{2+} homeostasis is still being clarified, the evidence for the existence of CIF continues to accumulate.

We thank Diane Weigent for excellent editorial work.

This work was supported in part by National Institutes of Health Grants AI-37670, MH-52527, and NS-29719 (to J. E. Blalock) as well as DK-55647 (to R. B. Marchase and J. E. Blalock); a Fifty 50 Food Juvenile Diabetes Foundation International Program Project Grant (to R. B. Marchase); Juvenile Diabetes Foundation Grant 2000-137 (to R. B. Marchase and J. E. Blalock); and a grant from the C. C. Wu Foundation in Hong Kong (to Z. Su).

REFERENCES

1. **Berridge MJ.** Inositol trisphosphate and calcium signalling. *Nature* 361: 315–325, 1993.
2. **Boulay G, Zhu X, Peyton M, Jiang M, Hurst R, Stefani E, and Birnbaumer L.** Cloning and expression of a novel mammalian homolog of *Drosophila* transient receptor potential (Trp) involved in calcium entry secondary to activation of receptors coupled by the G_q class of G protein. *J Biol Chem* 272: 29672–29680, 1997.
3. **Braun FJ, Broad LM, Armstrong DL, and Putney JWJ.** Stable activation of single Ca^{2+} release-activated Ca^{2+} channels in divalent cation-free solutions. *J Biol Chem* 276: 1063–1070, 2000.
4. **Chyb S, Raghu P, and Hardie RC.** Polyunsaturated fatty acids activate the *Drosophila* light-sensitive channels TRP and TRPL. *Nature* 397: 255–259, 1999.
5. **Clapham DE.** Calcium signaling. *Cell* 80: 259–268, 1995.
6. **Csutora P, Su Z, Kim HY, Bugrim A, Cunningham KW, Nuccitelli R, Keizer JE, Hanley MR, Blalock JE, and Marchase RB.** Calcium influx factor is synthesized by yeast and mammalian cells depleted of organellar calcium stores. *Proc Natl Acad Sci USA* 96: 121–126, 1999.
7. **Fierro L and Parekh AB.** On the characterisation of the mechanism underlying passive activation of the Ca^{2+} release-activated Ca^{2+} current I_{CRAC} in rat basophilic leukaemia cells. *J Physiol (Lond)* 520: 407–416, 1999.
8. **Garcia RL and Schilling WP.** Differential expression of mammalian TRP homologues across tissues and cell lines. *Biochem Biophys Res Commun* 239: 279–283, 1997.
9. **Gillo B, Chorna I, Cohen H, Cook B, Manistersky I, Chorev M, Arnon A, Pollock JA, Selinger Z, and Minke B.** Coexpression of *Drosophila* TRP and TRP-like proteins in *Xenopus* oocytes reconstitutes capacitative Ca^{2+} entry. *Proc Natl Acad Sci USA* 93: 14146–14151, 1996.
10. **Harootunian AT, Kao JP, Eckert BK, and Tsien RY.** Fluorescence ratio imaging of cytosolic free Na^{+} in individual fibroblasts and lymphocytes. *J Biol Chem* 264: 19458–19467, 1989.
11. **Hofmann T, Obukhov AG, Schaefer M, Harteneck C, Gudermann T, and Schultz G.** Direct activation of human TRPC6 and TRPC3 channels by diacylglycerol. *Nature* 397: 259–263, 1999.
12. **Hurst RS, Zhu X, Boulay G, Birnbaumer L, and Stefani E.** Ionic currents underlying HTRP3 mediated agonist-dependent Ca^{2+} influx in stably transfected HEK293 cells. *FEBS Lett* 422: 333–338, 1998.
13. **Kiselyov K and Muallem S.** Fatty acids, diacylglycerol, Ins(1,4,5)P3 receptors and Ca^{2+} influx. *Trends Neurosci* 22: 334–337, 1999.
14. **Kiselyov K, Xu X, Mozhayeva G, Kuo T, Pessah I, Mignery G, Zhu X, Birnbaumer L, and Muallem S.** Functional interaction between InsP3 receptors and store-operated Htrp3 channels. *Nature* 396: 478–482, 1998.

15. **Krause E, Pfeiffer F, Schmid A, and Schulz I.** Depletion of intracellular calcium stores activates a calcium conducting nonselective cation current in mouse pancreatic acinar cells. *J Biol Chem* 271: 32523–32528, 1996.
16. **Ma HT, Patterson RL, van Rossum DB, Birnbaumer L, Mikoshiba K, and Gill DL.** Requirement of the inositol trisphosphate receptor for activation of store-operated Ca^{2+} channels. *Science* 287: 1647–1651, 2000.
17. **Nofer J, Junker R, Seedorf U, Assmann G, Zidek W, and Tepel M.** D609-phosphatidylcholine-specific phospholipase C inhibitor attenuates thapsigargin-induced sodium influx in human lymphocytes. *Cell Signal* 12: 289–296, 2000.
18. **Nofer JR, Junker R, Walter M, Seedorf U, Assmann G, Zidek W, and Tepel M.** Phospholipase A_2 is involved in thapsigargin-induced sodium influx in human lymphocytes. *Arch Biochem Biophys* 374: 213–221, 2000.
19. **Parekh AB, Fleig A, and Penner R.** The store-operated calcium current I_{CRAC}: nonlinear activation by $InsP_3$ and dissociation from calcium release. *Cell* 89: 973–980, 1997.
20. **Patterson RL, van Rossum DB, and Gill DL.** Store-operated Ca^{2+} entry: evidence for a secretion-like coupling model. *Cell* 98: 487–499, 1999.
21. **Philipp S, Cavalie A, Freichel M, Wissenbach U, Zimmer S, Trost C, Marquart A, Murakami M, and Flockerzi V.** A mammalian capacitative calcium entry channel homologous to *Drosophila* TRP and TRPL. *EMBO J* 15: 6166–6171, 1996.
22. **Philipp S, Hambrecht J, Braslavski L, Schroth G, Freichel M, Murakami M, Cavalie A, and Flockerzi V.** A novel capacitative calcium entry channel expressed in excitable cells. *EMBO J* 17: 4274–4282, 1998.
23. **Putney JWJ.** Type 3 inositol 1,4,5-trisphosphate receptor and capacitative calcium entry. *Cell Calcium* 21: 257–261, 1997.
24. **Putney JWJ and Bird GS.** The signal for capacitative calcium entry. *Cell* 75: 199–201, 1993.
25. **Randriamampita C and Tsien RY.** Emptying of intracellular Ca^{2+} stores releases a novel small messenger that stimulates Ca^{2+} influx. *Nature* 364: 809–814, 1993.
26. **Randriamampita C and Tsien RY.** Degradation of a calcium influx factor (CIF) can be blocked by phosphatase inhibitors or chelation of Ca^{2+}. *J Biol Chem* 270: 29–32, 1995.
27. **Rudolph HK, Antebi A, Fink GR, Buckley CM, Dorman TE, LeVitre J, Davidow LS, Mao JI, and Moir DT.** The yeast secretory pathway is perturbed by mutations in PMR1, a member of a Ca^{2+} ATPase family. *Cell* 58: 133–145, 1989.
28. **Rzigalinski BA, Willoughby KA, Hoffman SW, Falck JR, and Ellis EF.** Calcium influx factor, further evidence it is 5, 6-epoxyeicosatrienoic acid. *J Biol Chem* 274: 175–182, 1999.
29. **Tepel M, Kuhnapfel S, Theilmeier G, Teupe C, Schlotmann R, and Zidek W.** Filling state of intracellular Ca^{2+} pools triggers trans plasma membrane Na^+ and Ca^{2+} influx by a tyrosine kinase-dependent pathway. *J Biol Chem* 269: 26239–26242, 1994.
30. **Trepakova ES, Csutora P, Hunton DL, Marchase RB, Cohen RA, and Bolotina VM.** Calcium influx factor (CIF) directly activates store-operated cation channels in vascular smooth muscle cells. *J Biol Chem* 275: 26158–26163, 2000.
31. **Vaca L, Sinkins WG, Hu Y, Kunze DL, and Schilling WP.** Activation of recombinant *trp* by thapsigargin in Sf9 insect cells. *Am J Physiol Cell Physiol* 267: C1501–C1505, 1994.
32. **Yao Y, Ferrer-Montiel AV, Montal M, and Tsien RY.** Activation of store-operated Ca^{2+} current in *Xenopus* oocytes requires SNAP-25 but not a diffusible messenger. *Cell* 98: 475–485, 1999.
33. **Zhu X, Jiang M, and Birnbaumer L.** Receptor-activated Ca^{2+} influx via human Trp3 stably expressed in human embryonic kidney (HEK)293 cells. Evidence for a non-capacitative Ca^{2+} entry. *J Biol Chem* 273: 133–142, 1998.
34. **Zhu X, Jiang M, Peyton M, Boulay G, Hurst R, Stefani E, and Birnbaumer L.** *trp*, a novel mammalian gene family essential for agonist-activated capacitative Ca^{2+} entry. *Cell* 85: 661–671, 1996.
35. **Zitt C, Obukhov AG, Strubing C, Zobel A, Kalkbrenner F, Luckhoff A, and Schultz G.** Expression of TRPC3 in Chinese hamster ovary cells results in calcium-activated cation currents not related to store depletion. *J Cell Biol* 138: 1333–1341, 1997.
36. **Zitt C, Zobel A, Obukhov AG, Harteneck C, Kalkbrenner F, Luckhoff A, and Schultz G.** Cloning and functional expression of a human Ca^{2+}-permeable cation channel activated by calcium store depletion. *Neuron* 16: 1189–1196, 1996.